JOURNAL OF MECHANICAL ENGINEERING AND SCIENCES (JMES)
ISSN: 2289-4659 e-ISSN: 2231-8380
VOL. 15, ISSUE 1, 7637 – 7647
DOI: https://doi.org/10.15282/jmes.15.1.2021.02.0602

ORIGINAL ARTICLE

Film cooling modeling of a gas turbine blade by considering different injection holes with and without opening angles through CFD

E. Hosseini[1]

[1] Department of Mechanical Engineering, Dezful Branch, Islamic Azad University, Dezful, Iran

ABSTRACT – One way to achieve high performance in the gas turbine is to increase the inlet temperature of the turbine. Different cooling techniques have been carried out in order to protect the turbine blades which have been exposed to such high temperatures. Film cooling as an essential cooling method needs to be enhanced to meet the challenging demand. The purpose of the present research is to analyze the film cooling performance over a NACA 0012 gas turbine blade using six different injection holes with and without opening angles, separately through Computational Fluid Dynamics (CFD). 2D Reynolds-Averaged Navier-Stokes (RANS) equations are implemented to consider the heat transfer and flow characteristics by using CFD code Ansys Fluent v16. The flow is considered as steady, turbulent, and incompressible. The RANS equation is solved with the finite-volume method for obtaining solutions. The simulation results revealed that the k-ω SST turbulence model is suitable for simulating the flow characteristics and analyzing the performance of film cooling over the blade. Also, the opening angle has a significant effect on increasing the cooling efficiency for the upper blade surface. The highest value of cooling efficiency is obtained by the injection hole with an opening angle of 15° and height of D. In this configuration, the coolant injected from hole provides better cooling coverage for the entire blade which increases the cooling effectiveness.

ARTICLE HISTORY
Received: 21st Aug 2020
Revised: 21st Jan 2021
Accepted: 17th Feb 2021

KEYWORDS
Film cooling;
CFD;
Cooling efficiency;
Injection holes;
NACA 0012

INTRODUCTION

Nowadays, due to the increasing use of gas turbine applications in power plants and aerospace industries, more attention has been paid to improve the performance and eliminating the shortcomings of this equipment. One way to achieve high performance in gas turbines is the increment of the turbine inlet temperature. Thus, methods for cooling components that are damaged from heat, have been investigated by researchers. The gas turbine engine utilizes cooling methods for keeping metal components within allowable operational temperature ranges because of exceptionally high turbine inlet temperature. Film cooling as one of the capable cooling techniques is implemented for the gas turbine blade [1]. The turbine inlet temperatures become higher for improving the efficiency of turbine engines that makes it far higher than the melting point of the turbine blade. Hence, it is essential for decreasing the heat load and ensuring the safe operation of the blades by cooling the blade of the gas turbine [2]. The effect of film cooling on the performance of blades is becoming significantly important when the temperature of the gas turbine is raised to enhance its performance [3-5]. Computational Fluid Dynamics (CFD) has now found its place among experimental and analytical methods for analyzing fluid flow, heat transfer [6-13], and diverse problems [14-16], and the use of this method for engineering analysis has become more common [17-20].

Several numerical and experimental works have been done to analyze the influence of film cooling on gas turbine performance. Nowadays, the CFD prediction of the film cooling method is a valuable part of designing the process of the cooling scheme for gas turbines [21,22]. The infrared thermography was utilized in the study of Kim et al. [23] to analyze the impact of different injection holes over a gas turbine blade for film cooling. They noted that the shaped holes can significantly enhance the performance of film cooling. Li et al. [24,25] experimentally measured the effects of Reynolds number and blowing on a blade of the turbine. They stated that the average film cooling efficiency improved by increasing Reynolds number (at a fixed blowing ratio). Lanzillotta et al. [3] studied the effect of the blowing ratio on the aerodynamic performance of the turbine blade. They concluded that the separation point moves upstream (low blowing ratios), and the coolant energizes the flow and postponed the flow separation (high blowing ratios). Cao et al. [26] experimentally and numerically analyzed four different film holes to consider the impact of hole geometry and blowing ratio on the efficiency of film cooling. The results indicated that the sister hole shows the best cooling performance. Han et al. [27] measured the impacts of the hole pitch and the blowing ratio on the film cooling characteristics of a gas turbine blade. They demonstrated that both the hole pitch and the blowing ratio play a major role to determine the film cooling efficiency. Zhou et al. [28] studied the heat transfer performances of the sister holes cooling schemes using a numerical method. They concluded that the best performance of film cooling for sister holes cooling cases was achieved with the smallest diameter ratio. Yang et al. [29] numerically evaluated the overall efficiency of the cooling film for the adiabatic efficiency of the film cooling and the heat transfer coefficient. By increasing the blowing ratios, the three holes provide better

*CORRESPONDING AUTHOR | E. Hosseini | ✉ ebrahim.2019.hosseini@gmail.com

cooling efficiency. Meanwhile, bean-shaped holes indicated maximum efficiency among the other shapes. Garcia et al. [30] optimized the performance of film cooling over the leading edge of a gas turbine blade using differential evolution. They showed that the coolant flow rate was decreased by about 66% and the cooling efficiency was enhanced by about 36% after optimizing the cooling holes. Dickhoff et al. [31] numerically simulated the film cooling process using different holes and compared two different isotropic and anisotropic eddy viscosity, models. In their study, in addition to the conventional shape of the hole, nekomimi holes were implemented.

In this study, an attempt is made to numerically consider the effect of film cooling on the NACA 0012 gas turbine blade. For this purpose, six different injection holes with and without opening angles are considered, separately. Six different cases of film cooling are analyzed to find the appropriate injection hole with favorable geometry for the film cooling process. Several numerical simulations are conducted through the CFD method to provide a comprehensive performance of film cooling of new cooling hole shapes with opening angles.

COMPUTATIONAL DOMAIN

Figure 1 depicts the two-dimensional computational domain for the present research. The chord (c) length of the NACA 0012 airfoil is 1000 mm and the diameter of the injection hole is 20 mm which is denoted by D. The computational domain is extended from 5c upstream to 15c downstream and the upper boundary and lower boundary are extended 5c from the airfoil. No-slip wall condition is set over the airfoil surface. The velocity inlet boundary condition is applied at the inlet, the upper boundary, and the lower boundary, while the pressure outlet boundary condition is imposed at the outlet. A C-type structured grid is implemented for the computational domain as illustrated in Figure 1. Two injection angles of 15° and 20° are used for the injection holes with opening angles. More details of injection holes are presented in Table 1. The schematic views of six different cases of film cooling holes are demonstrated in Figure 2.

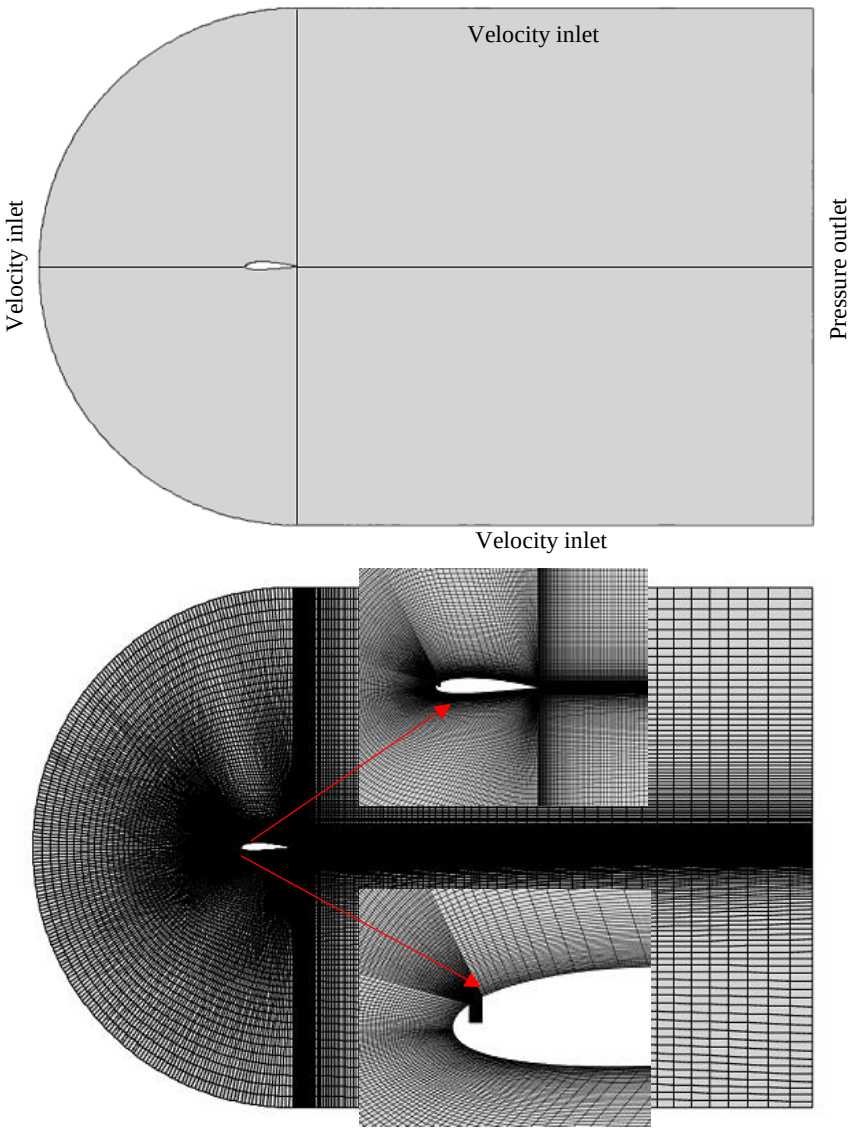

Figure 1. Computational domain and boundary conditions

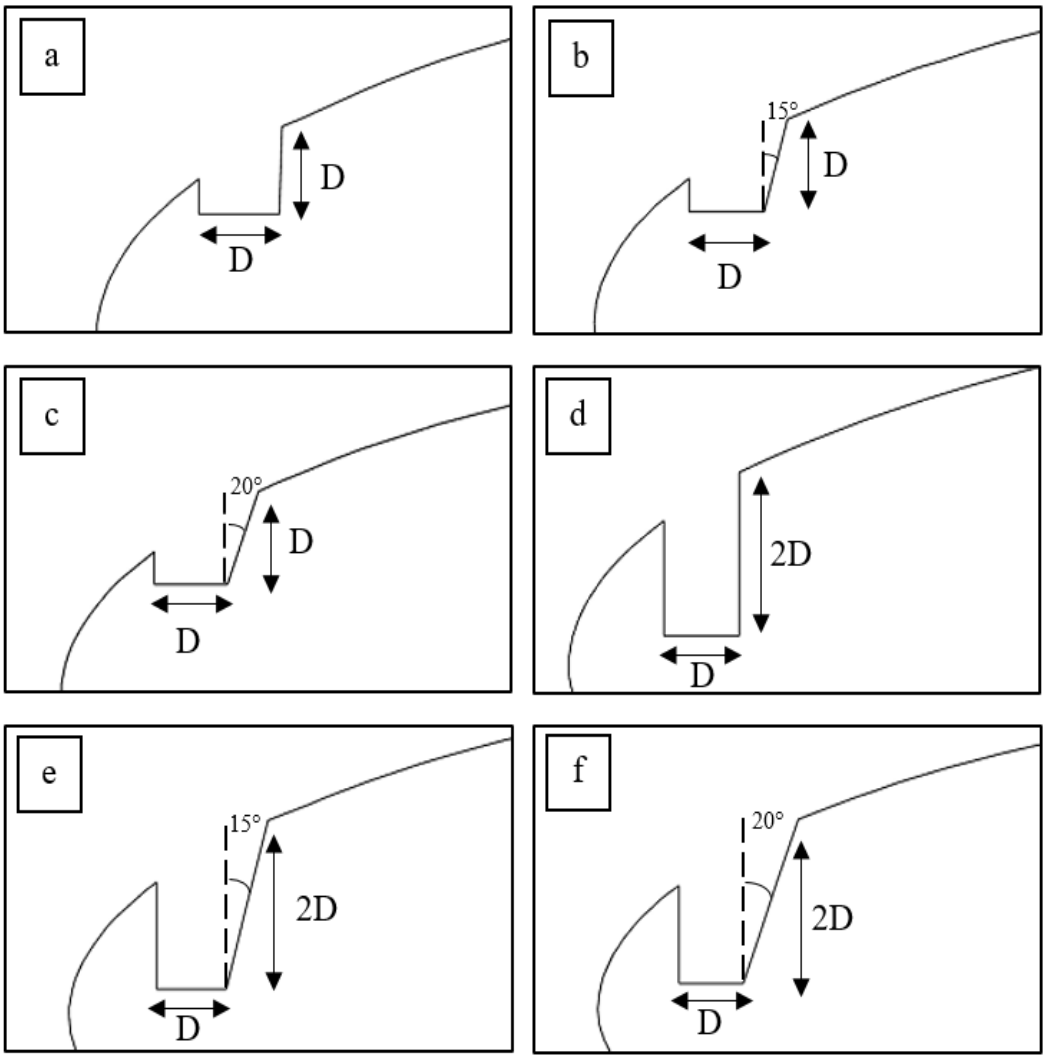

Figure 2. Schematic views of injection holes, namely: (a) Case 1, (b) Case 2, (c) Case 3, (d) Case 4, (e) Case 5 and (f) Case 6

Table 1. Different cases of injection holes

Case	Width	Height	Angle (°)
1	D	D	0
2	D	D	15
3	D	D	20
4	D	2D	0
5	D	2D	15
6	D	2D	20

MATHEMATICAL FORMULATION

In the present study, the steady-state incompressible RANS equation is solved by a commercial CFD solver, Ansys Fluent v16. The RANS equation is solved with a finite-volume method for obtaining solutions [32-34]. The continuity, momentum, and energy equations are solved. The SST k-ω turbulence model is employed to simulate the turbulent flow which is more accurate for the considered flow. This model can be written as [35]:

$$\frac{\partial}{\partial t}(\rho k)+\frac{\partial}{\partial x_i}(\rho k u_i)=\frac{\partial}{\partial x_j}\left[\Gamma_k\frac{\partial k}{\partial x_j}\right]+G_k-Y_k \tag{1}$$

$$\frac{\partial}{\partial t}(\rho \omega)+\frac{\partial}{\partial x_i}(\rho \omega u_i)=\frac{\partial}{\partial x_j}\left[\Gamma_\omega\frac{\partial \omega}{\partial x_j}\right]+G_\omega-Y_\omega+D_\omega \tag{2}$$

where Γ_k and Γ_ω indicate the effective diffusivity of k and ω, respectively. G_k and G_ω show the generation of k and ω due to mean velocity gradients, respectively. Y_k and Y_ω denote the dissipation of k and ω, respectively. D_ω is the cross-diffusion term of ω [36,37].

The operating fluid, as well as the cooling fluid, are both considered as the air. Due to the low-temperature difference (20° C) between the main flow and injection flow, the ratio of cold and hot air densities is assumed to be equal. Hence, the assumption of the blowing ratio is described as the ratio of the injection velocity to the free stream velocity [21]:

$$BR=\frac{\rho_c V_c}{\rho_\infty V_\infty}=\frac{V_c}{V_\infty} \tag{3}$$

where V_c denotes the injection velocity, V_∞ denotes the free stream velocity and ρ represents the density. The inlet flow velocity is 70 m/s in the x-direction and T_∞ = 300 k. For the injection coolant air, the velocity is assumed to be 70 m/s at T_c = 280 k, by considering the blowing ratio equal to 1. The outlet pressure is equal to atmospheric pressure 101325 Pa. The upwind second-order method is implemented for the discretization of equations. Also, The SIMPLE algorithm is used for pressure-velocity coupling. For all equations, the convergence criteria are considered to be less than 10^{-5}. The boundary layer regions for all walls are refined to ensure values of y^+ less than 1.

CODE VALIDATION

The grid specifications and y^+ distribution at α = 10° are presented in Table 2. Besides, y^+ distribution over NACA 0012 airfoil at α = 10° is illustrated in Figure 3. The value of y^+ is kept at less than 1 by considering that the distance of the nearest node from the airfoil surface is 1×10^{-5} (m) [38]. The grid independence study is carried out to calculate the drag coefficient (C_D) of the NACA 0012 airfoil at α = 10° and α = 16°. Different grids with cell numbers of 35144, 43980, 52200, and 65347 are generated to investigate the grid independence (Figure 4). There is a negligible difference between the results of the smallest grid and the grid with 52200 cells. Hence, 52200 cells have a grid-independent result with reasonable accuracy. Three different computational domains are generated to consider the drag coefficient (C_D) for the domain extent independence test, as shown in Table 3. It is observed that the second domain is appropriate for the present simulation.

Table 2. y^+ Distribution at α = 10° and grid specifications

Grid	Cell number	Growth factor	Height of the first cell (m)	Max y+	Min y+	Average y+
1	18000	1.1	2×10^{-3}	14.11	3.41	8.12
2	32000	1.1	1×10^{-4}	6.12	0.85	2.93
3	46000	1.1	1×10^{-5}	0.81	0.02	0.26
4	65000	1.1	3×10^{-6}	0.63	0.01	0.21

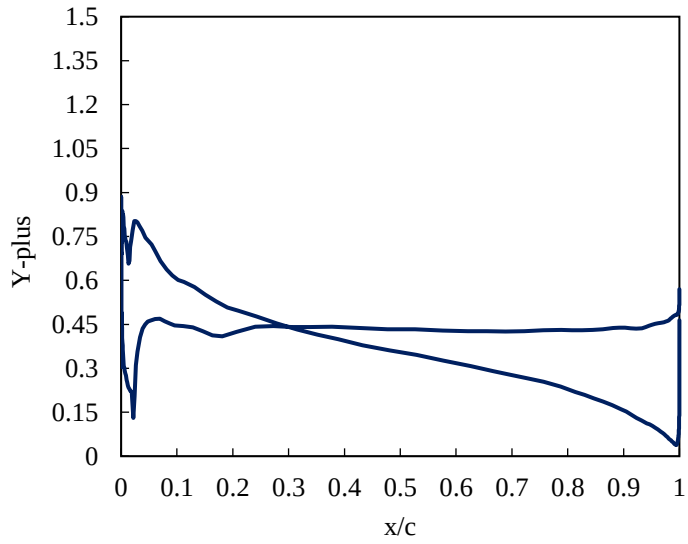

Figure 3. y^+ distribution over NACA 0012 airfoil at a = 10°

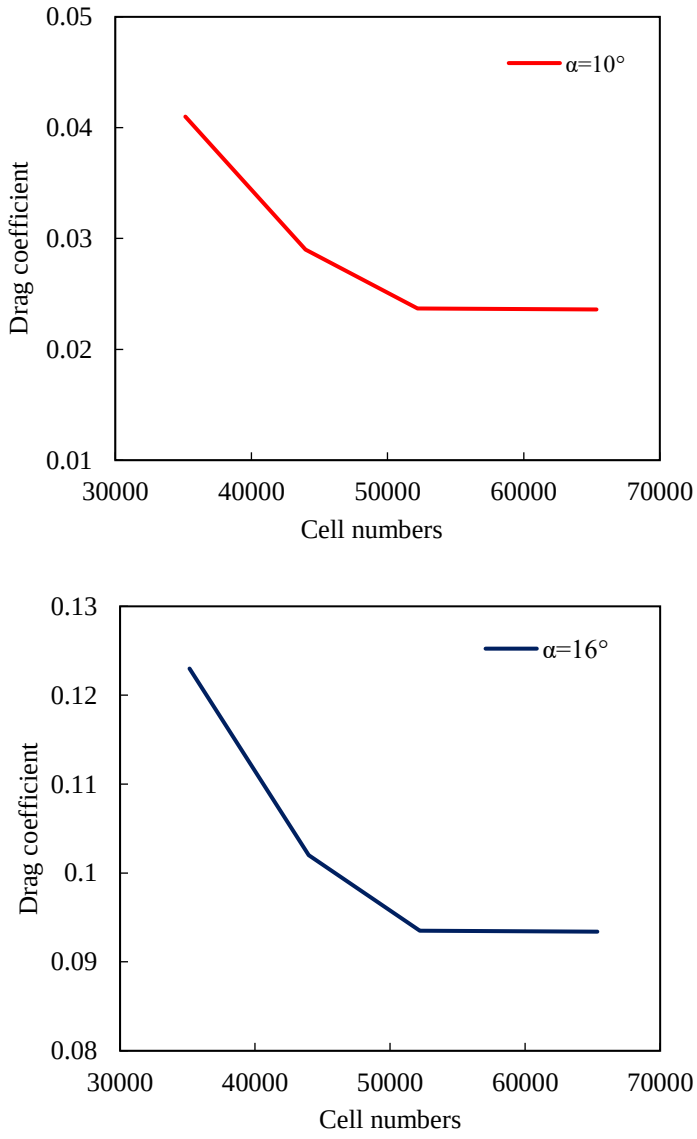

Figure 4. Grid independence study

Table 3. Domain independence test

Size	Upstream	Downstream	C_D
1	4 c	12 c	0.0259
2	5 c	15 c	0.0237
3	6 c	18 c	0.0235

As shown in Figure 5, the computational result of the pressure coefficient is compared with the experimental results of Gregory and O'reilly [39] for a NACA 0012 airfoil at a Reynolds number of 5×10^5 and $\alpha = 18°$. The numerical validation is done with several turbulence models: k-ε, RNG k-ε, and SST k-ω. Generally, the SST k-ω turbulence model presents better agreement with the experimental results. Hence, it was found that the numerical method has acceptable accuracy.

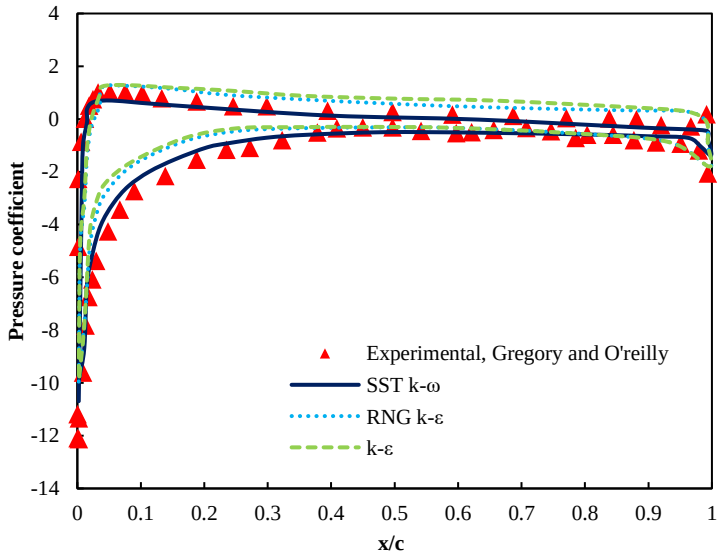

Figure 5. Validation

RESULTS AND DISCUSSIONS

Figure 6 demonstrates the temperature distribution (k) over the blade for all cases. In this figure, six different cases for the film cooling process are compared. For all cases, the high cooling effectiveness regions achieved just downstream of the film hole exit. It can be seen, for an injection hole with a 15° opening angle (case 2), the coolant spread is much better than the other cases. The coolant coverage is quite uniform on the upper side of the blade. This revealed that this cooling hole has enough resistance to the impact of main flow acceleration and adverse pressure gradient produced by concave curvature of the surface near the trailing edge. Using an injection hole with a 15° opening angle leads to minimize the recirculation zone after the injection hole.

The velocity contours around the blade for different cases are illustrated in Figure 7. A similar effect of cooling air on the velocity flow field is observed. The injection hole with an opening angle positively reduces the recirculation zone after exiting of coolant. This causes to accelerate the flow over the blade surface and increase the momentum deficit in the wake results in a reduction of the negative effect of the adverse pressure gradient. This is more evident in case 2 in which the flow around the blade is energized caused by the momentum of injected coolant and so the flow stays attached to the upper surface.

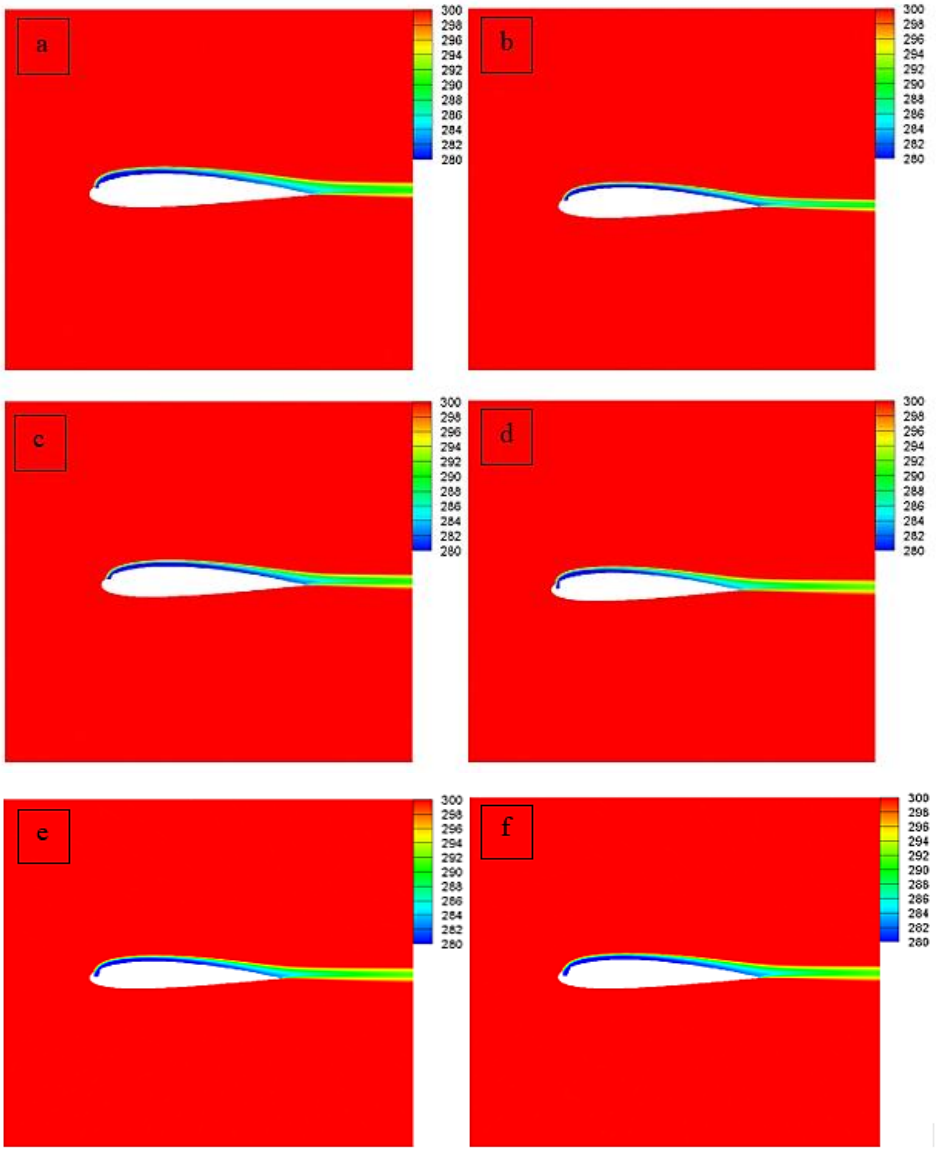

Figure 6. Temperature distribution (k) over the blade: (a) Case 1, (b) Case 2, (c) Case 3, (d) Case 4, (e) Case 5 and (f) Case 6

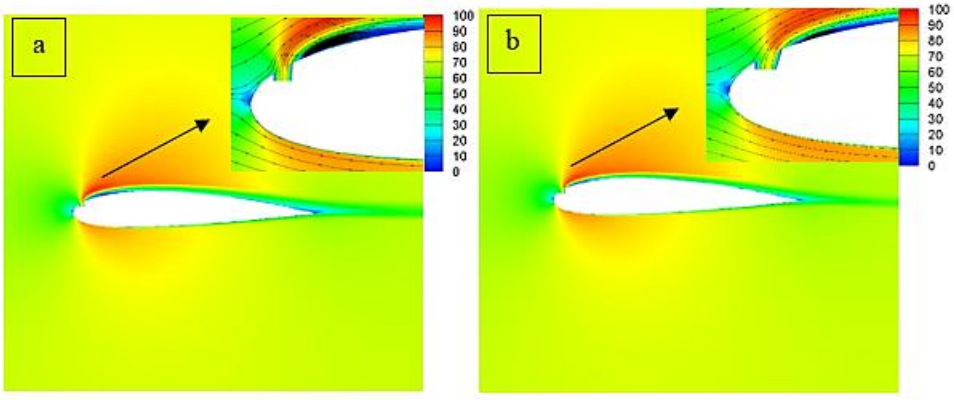

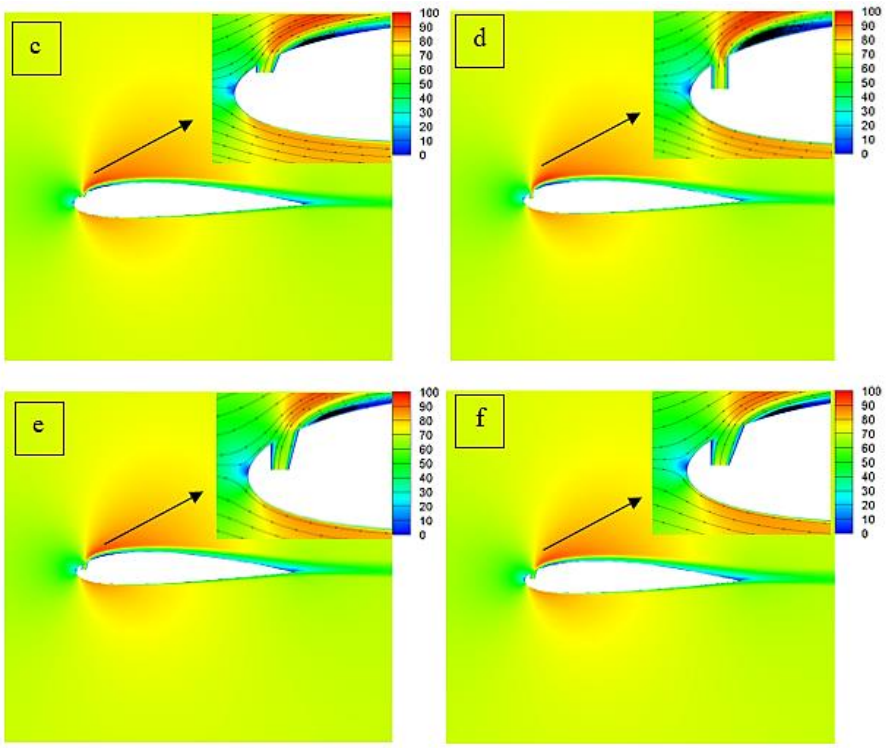

Figure 7. Velocity contours (m/s) and flow pattern around the blade: (a) Case 1, (b) Case 2, (c) Case 3, (d) Case 4, (e) Case 5 and (f) Case 6

Figure 8 illustrates the comparison of temperature distribution over the upper surface of the blade for different cases. It was found that the injection hole with an opening angle performs better than without opening angle holes. The maximum reduction of temperature is obtained by case 2 which indicates that more coolant is carried by the secondary flow to concentrate over the upper surface of the blade. It is obvious that shaping the injection hole with an opening angle provides better film cooling on the blade. Increasing the height of the injection hole is detrimental to the cooling process whereas it reduces the exit momentum of the coolant and worsens the attachment to the blade surface. These seem to cause less coolant to be entrained and carried to the leading edge by secondary flows.

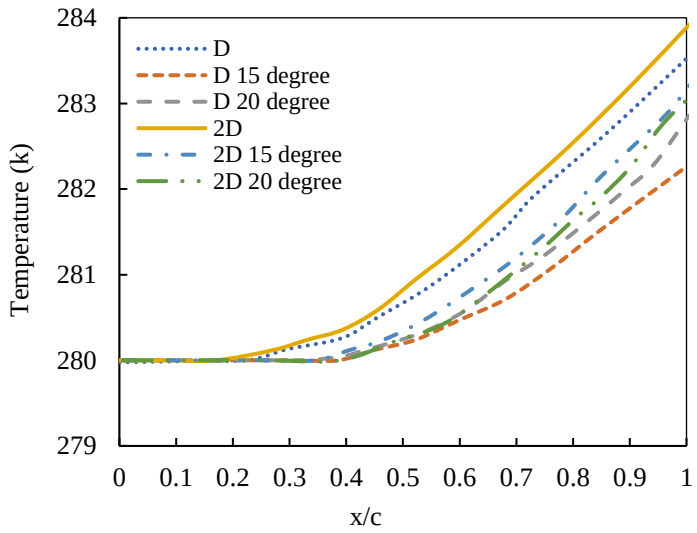

Figure 8. Temperature distribution over the blade for different cases

Figure 9 depicts the comparison of the cooling efficiency for different cases. The adiabatic film cooling efficiency (η) can be written as [26]:

$$\eta = \frac{T_m - T_{aw}}{T_m - T_c} \tag{4}$$

where T_m denotes the mainstream temperature, T_{aw} is the adiabatic wall temperature, and T_c represents the coolant temperature. The process of film cooling generally depends on interactions between the injected coolant-streams and passage secondary flows. The maximum film cooling effectiveness is observed at the leading edge of the airfoil and decreases steadily downstream for all cases. It is clear that the injection holes with opening angles have a positive effect on increasing the cooling efficiency. The maximum value of cooling efficiency is obtained for case 2. In this case, the coolant injected from case 2 provides better cooling coverage for the entire blade which increases cooling effectiveness.

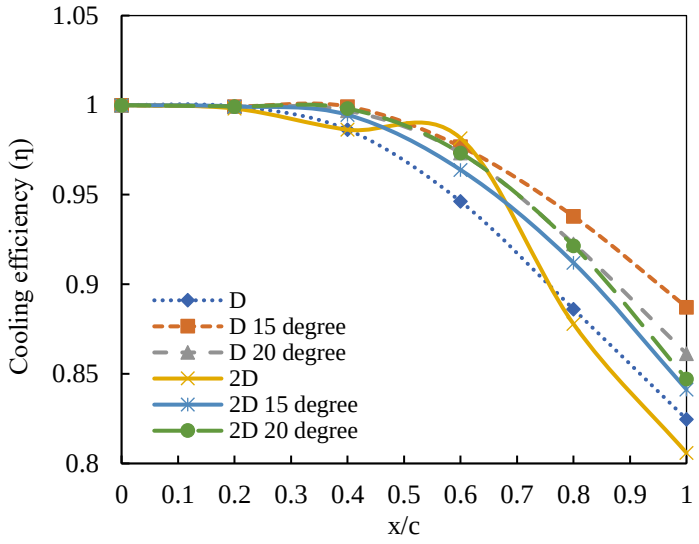

Figure 9. The comparison of cooling efficiency of injection holes for different cases

CONCLUSIONS

The main purpose of the present work is to analyze the film cooling process on an asymmetric NACA 0012 gas turbine blade using injection holes using CFD modeling. Also, the performance of injection holes with different geometries on the effectiveness of film cooling has been numerically investigated. For this purpose, six different injection holes with and without opening angles are considered, separately. By comparing the temperature distribution over the airfoil surface for all cases, it was concluded that as the injection hole has a lower height, it has a better impact on the cooling efficiency of the upper surface of the blade compared to other cases. Also, the lower opening angle has more effect on the film cooling than the larger opening angle. Furthermore, the film cooling process commonly depends on interactions between the injected coolant-streams and passage secondary flows. The injection hole with an opening angle positively reduces the recirculation zone after exiting of coolant. In this way, the accelerated flow with higher momentum uniformly spread over the blade which led to decrease the negative effect of the adverse pressure gradient.

REFERENCES

[1] F. Fan, C. Wang, J. Zhang, "Large eddy simulation of film cooling on turbine vane," *J. Therm. Sci.Tech.*, vol. 14, pp. 1-12, 2019.

[2] S. Mathew, S. Ravelli, D. Bogard, "Evaluation of CFD predictions using thermal field measurements on a simulated film cooled turbine blade leading edge," *J. Turbomach.*, vol. 135, pp. 1-15, 2013.

[3] F. Lanzillotta, A. Sciacchitano, A. Rao, "Effect of film cooling on the aerodynamic performance of an airfoil," *Int. J. Heat Fluid Fl.*, vol. 66, pp. 108-120, 2017.

[4] A. S. Shote, G. I. Mahmood, J. P. Meyer, "Influences of large fillets on endwall flows in a vane cascade with upstream slot film-cooling," *Exp. Therm. Fluid Sci.*, vol. 112, pp. 1-12, 2020.

[5] Z. Yu, C. Li, B. An, J. Liu, G. Xu, "Experimental investigation of film cooling effectiveness on a gas turbine blade pressure surface with diffusion slot holes," *Appl. Therm. Eng.*, vol. 168, pp. 1-18, 2020.

[6] S. B. Ahangar, J. S. Allen., S. H. Lee, C. K. Choi, "Surface Plasmon Resonance Imaging: A Technique to Reveal the Dropwise Condensation Mechanism," *J. Heat Transf.*, vol. 142, pp. 030903, 2020.

[7] S. B. Ahangar, V. Konduru, J. S. Allen, N. Miljkovic, S. H. Lee, C. K. Choi, "Development of automated angle-scanning, high-speed surface plasmon resonance imaging and SPRi visualization for the study of dropwise condensation," *Exp. Fluids*, vol. 61, pp. 12-20, 2020.

[8] S. B. Ahangar, C. H. Jeong, F. Long, J. S. Allen, S. H. Lee, C. K. Choi, "The Effect of Adsorbed Volatile Organic Compounds on an Ultrathin Water Film Measurement," *Appl. Sci.*, vol. 10, pp. 5981, 2020.

[9] S. Bayani, Y. Tabe, Y. T. Kang, S. H. Lee, C. K. Choi, "Surface plasmon resonance imaging of drop coalescence at high-temporal resolution," *J. Flow Image Process.*, vol, 25, pp. 191-205, 2018.

[10] M. Rahim-Esbo, S. Bayani, R. Mohammadyari, A. K. Asboei, S. Mohsenian, S. E. Mousavitileboni, "Analytical and Numerical investigation of natural convection in a heated cylinder using Homotopy Perturbation Method," *Acta Sci-Technol.*, vol. 36, pp. 669-677, 2014.

[11] N. M. Nouri, S. Sekhavat, S. Bayani Ahangar, N. Faal Nazari, "Effect of curing condition on superhydrophobic surface for 7075Al," *J. Disper. Sci. Technol.*, vol. 33, pp. 771-774, 2012.

[12] H. Fatahian, E. Fatahian, "Improving efficiency of a square cyclone separator using a dipleg–a CFD-based analysis," *IRAN J. Chem. Chem. Eng.*, 2020, doi: 10.30492/ijcce.2020.127666.4129.

[13] E. Fatahian, H. Salarian, H. Fatahian, "Numerical Investigation of Hazardous Gas Dispersion Over Obstacles and Residential Areas," *Int. J. Eng.*, vol. 33, pp. 2087-2094, 2020.

[14] H. Fatahian, E. Hosseini, E. Fatahian, "CFD simulation of a novel design of square cyclone with dual-inverse cone," *Adv.Powder Technol.*, vol. 31, pp. 1748-1758, 2020.

[15] X. Yang, Q. Zhao, Z. Liu, Z. Feng, "Film Cooling Patterns over an Aircraft Engine Turbine Endwall with Slot Leakage and Discrete Hole Injection," *Int. J. Heat Fluid Fl.*, vol. 165, pp. 120565, 2021.

[16] E. Fatahian, H. Fatahian, "CFD modeling of the effect of dipleg geometry on improving efficiency of a square cyclone," *AUT J. Mech. Eng.*, 2021, doi: 10.22060/ajme.2021.18498.5902.

[17] R. Zhu, E. Lin, T. Simon, G. Xie, "Investigation and numerical simulation on film cooling performance with an anti-vortex hole design: Influences of diameter ratio," *Int. Commun. Heat mass*, vol. 121, pp. 105118, 2021.

[18] J. Wang, L. Li, J. Li, F. Wu, C. Du, "Numerical investigation on flow and heat transfer characteristics of vortex cooling in an actual film-cooled leading edge," *Appl. Therm. Eng.*, vol. 185, pp. 115942, 2021.

[19] E. Fatahian, H. Salarian, H. Fatahian, "A parametric study of the heat exchanger copper coils used in an indirect evaporative cooling system," *SN Appl. Sci.*, vol. 2, pp. 1-10, 2020.

[20] H. Fatahian, H. Salarian, J. Khaleghinia, E. Fatahian, "Improving the efficiency of a Savonius vertical axis wind turbine using an optimum parameters," *Comput Res Prog Appl Sci Eng*, vol. 4, pp. 27-32, 2018.

[21] P. Chen, L. Wang, X. Li, J. Ren, H. Jiang, "Effect of axial turbine non-axisymmetric endwall contouring on film cooling at different locations," *Int. J. Heat Mass Tran.*, vol. 147, pp. 1-9, 2019.

[22] P. Chen, M. Alqefl, X. Li, J. Ren, H. Jiang, T. Simon, "Cooling effectiveness and aerodynamic performance in a 2D-Contoured endwall passage with different mass flow ratios," *International Journal of Thermal Sciences*, vol. 142, pp. 233-246, 2019.

[23] Y. J. Kim, S. M. Kim, "Influence of shaped injection holes on turbine blade leading edge film cooling," *Int. J. Heat Mass Tran.*, vol. 47, pp. 245-256, 2004.

[24] H. W. Li, F. Han, Z. Zhou, Y. Ma, Z. Tao, "Experimental investigations of the effects of the injection angle and blowing ratio on the leading-edge film cooling of a rotating twisted turbine blade," *Int. J. Heat Mass Tran.*, vol. 127, pp. 856-869, 2018.

[25] H.W. Li, F. Han, H. C. Wang, Z. Zhou, Z. Tao, "Film cooling characteristics on the leading edge of a rotating turbine blade with various mainstream Reynolds numbers and coolant densities," *Int. J. Heat Mass Tran.*, vol. 127, pp. 833-846, 2018.

[26] N. Cao, X. Li, Z. Wu, X. Luo, "Effect of film hole geometry and blowing ratio on film cooling performance," *Appl. Therm. Eng.*, vol. 165, pp. 1-10, 2020.

[27] F. Han, H. Guo, X. F. Ding, D. W. Zhang, H. W. Li, "Experimental investigation on the effects of hole pitch and blowing ratio on the leading edge region film cooling of a rotating twist turbine blade," *Int. J. Heat Mass Tran.*, vol. 150, pp. 1-12, 2020.

[28] J. Zhou, X. Wang, J. Li, H. Lu, "Effects of diameter ratio and inclination angle on flow and heat transfer characteristics of sister holes film cooling," *Int. Commun. Heat mass*, vol. 110, pp. 1-18, 2020.

[29] X. Yang, Z. Liu, Z. Feng, "Numerical evaluation of novel shaped holes for enhancing film cooling performance," *J. Heat Transf.*,, vol. 137, pp. 1-18, 2015.

[30] J. García, J. Dávalos, G. Urquiza, S. Galván, A. Ochoa, J. Rodríguez, C. Ponce, "Film cooling optimization on leading edge gas turbine blade using differential evolution," *P. I. Mech. Eng. G-J. Aer.*, vol. 233, pp. 1656-1666, 2019.

[31] J. Dickhoff, K. Kusterer, S. Bhaskar, D. Bohn, "CFD Simulations for Film Cooling Holes: Comparison Between Different Isotropic and Anisotropic Eddy Viscosity Models," In *Turbo Expo: Power for Land, Sea, and Air* (Vol. 51081, p. V05AT12A008). American Society of Mechanical Engineers, 2018.

[32] H. Fatahian, H. Salarian, M. E. Nimvari, J. Khaleghinia, "Effect of Gurney flap on flow separation and aerodynamic performance of an airfoil under rain and icing conditions," *Acta Mech. Sinica.*, vol. 36, pp. 659-677, 2020.

[33] H. Fatahian, H. Salarian, M. E. Nimvari, J. Khaleghinia, "Computational fluid dynamics simulation of aerodynamic performance and flow separation by single element and slatted airfoils under rainfall conditions," *Appl. Math. Model.*, vol. 83, pp. 683-702, 2020.

[34] E. Fatahian, A. L. Nichkoohi, H. Fatahian, "Numerical study of the effect of suction at a compressible and high Reynolds number flow to control the flow separation over Naca 2415 airfoil," *Prog. Comput. Fluid Dy.*, vol. 19, pp. 170-179, 2019.

[35] F. R. Menter, "Two-equation eddy-viscosity turbulence models for engineering applications," *AIAA J.*, vol. 32, pp. 1598-1605, 1994.

[36] E. Fatahian, A. L. Nichkoohi, H. Salarian, J. Khaleghinia, "Effects of the hinge position and suction on flow separation and aerodynamic performance of the NACA 0012 airfoil," *J. Braz. Soc. Mech. Sci.*, vol. 42, pp. 1-14, 2020.

[37] E. Fatahian, A. L. Nichkoohi, H. Salarian, J. Khaleghinia, "Comparative study of flow separation control using suction and blowing over an airfoil with/without flap," *Sādhanā*, vol. 44, pp. 220-229, 2019.

[38] H. K. Versteeg, W. Malalasekera, "*An introduction to computational fluid dynamics: the finite volume method*," Pearson education, London, 2007.

[39] N. Gregory, C. L. O'reilly, "Low-speed aerodynamic characteristics of NACA 0012 aerofoil section, including the effects of upper-surface roughness simulating hoar frost," HM Stationery Office, London, 1970.